J. Astrophys. Astr. (2018) 39:39
https://doi.org/10.1007/s12036-018-9527-4

Kelvin–Helmholtz instability of two finite-thickness fluid layers with continuous density and velocity profiles

G. A. HOSHOUDY[1,*] and HUSEYIN CAVUS[2]

[1]Department of Applied Mathematics, Faculty of Science, South Valley University, Kena 83523, Egypt.
[2]Physics Department, Arts and Science Faculty, Canakkale Onsekiz Mart University, 17100 Canakkale, Turkey.
*Corresponding author. E-mail: g_hoshoudy@yahoo.com

MS received 24 January 2018; accepted 7 May 2018; published online 19 June 2018

Abstract. The effect of density and velocity gradients on the Kelvin–Helmholtz instability (KHI) of two superimposed finite-thickness fluid layers are analytically investigated. The linear normalized frequency and normalized growth rate are presented. Then, their behavior as a function of the density ratio of the light fluid to the heavy one (r) was analyzed and compared to the case of two semi-infinite fluid layers. The results showed that the values of normalized frequency of KHI for two finite-thickness fluid layers are less than their counterparts for two semi-infinite fluid layers. The behavior of normalized growth rate as a function of the velocity and density gradients capitulates to the effect of velocity gradient at the large values of (r).

Keywords. Kelvin–Helmholtz—finite-thickness—density—velocity gradients.

1. Introduction

The Kelvin–Helmholtz instability (KHI) (Helmholtz 1868; Kelvin 1871) arises when the two fluids are initially in motion, and there is a variation across the interface of the velocity component parallel to the interface. A velocity shear leads to the creation of vortices which entrain the two fluids in a characteristic rotational motion. Alexakis *et al.* (2002) examined the linear stability of fluid interfaces subjected to a shear flow. A generalization for an arbitrary Atwood number together with surface tension and weak compressibility was studied. They provided the estimates of the growth rates of unstable surface waves. Chong *et al.* (2008) concentrated on a generalization of the classical KHI for a moving interface with taking into account the family of a continuous density profile and a continuous parallel velocity profile. They proposed a new growth rate expression. The KHI can also arise along the interface between the ascending bubbles and descending spikes of late-stage Rayleigh–Taylor instability (RTI), where the shear due to the differential motion of these structures can be significant. Raj and Guha (2017) investigated the effect of shear on the RTI. They found that, the uniform shear suppresses RTI for longer waves at higher values of Atwood number (large density stratification).

KHI is important in understanding a variety astrophysical phenomena involving sheared plasma flow (e.g., the stability of the solar wind-magnetosphere interface, interaction between adjacent streams of different velocities in the solar wind). Also, the KHI is ubiquitous high-energy density physics (HEDP), such as the high-Mach-number shocks and jets, radioactive blast waves and radioactively driven molecular clouds, gamma-ray bursts and accreting black holes (Remington *et al.* 2006; Harding & Hansen 2009; Harding *et al.* 2010). On the other hand, the KHI under high-energy-density (HED) has been extensively investigated experimentally (Drake 2005; Hurricane *et al.* 2009).

The instability of the interface separating two semi-infinite fluid layers has also been achieved by several

authors. For example, the detailed description of different parameters was given by Chandrasekhar (1961). The instability of the interface separating two finite-thickness fluid layers in the case of fluids filling a cavity which performs horizontal harmonic oscillations was considered by Khenner *et al.* (1999). The dielectric fluids with interfacial transfer of mass and heat for two layers of finite thickness have been studied by Mohamed *et al.* (1994).

Both the density and velocity gradients play an important role in the KHI. This role has also been studied for two semi-infinite fluid layers by Wang *et al.* (2009, 2010); Ye *et al.* (2011) and numerically has been presented by Gan *et al.* (2011). The results show that the density gradient enhances the linear growth rate of KHI, the velocity gradient reduces the linear growth rate of KHI, but cannot completely stabilize it. While, in most cases, the overall combined effects of density and velocity gradients tend to stabilize the KHI.

The combined effect of density and velocity gradients on KHI in the previous works have been studied of two semi-infinite fluid layers, but for two finite-thickness fluid layers are still not well understood, which maybe play major roles in the performance of the astrophysical jets and jet-like long spikes in the high-energy density physics (HEDP), also in the solar atmosphere (Zaqarashvili *et al.* 2015; Zhelyazkov 2015; Kuridze *et al.* 2016) and in the solar wind (Zaqarashvili *et al.* 2014). So, our aim in this letter is to discuss the combined effect of density and velocity gradients on the KHI of two finite-thickness fluid layers.

2. Fundamental equations

Our starting point will be with the general eigenvalue equation (Eq. 5) given by Wang *et al.* (2010), which we can be rewritten as

$$\begin{aligned}\frac{d}{dy}\left\{\frac{1}{k^2}\left\{\left[\rho^{(0)}\left(\sigma+iku^{(0)}(y)\right)\right]\left(-\frac{du_y}{dy}\right)\right.\right.\\ \left.\left.+\rho^{(0)}\left(ik\,u_y\frac{du^{(0)}(y)}{dy}\right)\right\}\right\}\\ =-\rho^{(0)}\left(\sigma+ik\,u^{(0)}(y)\right)u_y\\ +\frac{g}{\sigma+ik\,u^{(0)}(y)}\frac{d\rho^{(0)}(y)}{dy}u_y \qquad (1)\end{aligned}$$

where $\sigma=\gamma-i\omega$(σ denotes the rate at which the system departs from equilibrium), γ and ω are linear growth rate and the frequency of perturbations, respectively.

For two superimposed finite-thickness fluid layers (see Fig. 1), we will integrating Eq. (1) over $-h<y<+h$.

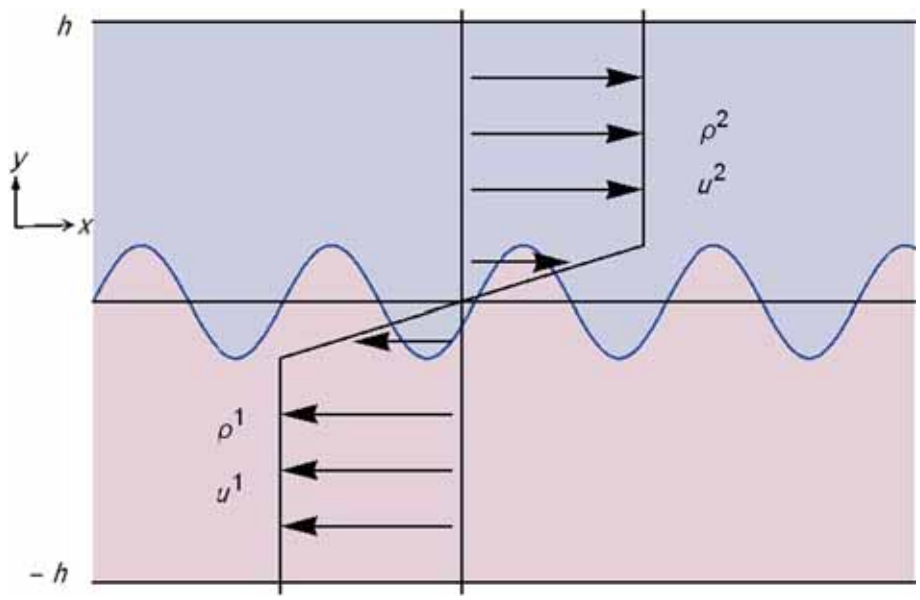

Figure 1. Schematic diagram of two finite-thickness fluid layers with continuous density and velocity profiles.

Also, we let the profiles of density and velocity are exponential functions in $y-$direction, respectively, as

$$\rho^0(y) = \begin{cases} \rho_h - \frac{\Delta\rho}{2}\frac{\cosh\frac{1}{kL_\rho}(kh-ky)}{\cosh\frac{kh}{kL_\rho}}, & 0 \le y \le h \\ \rho_l + \frac{\Delta\rho}{2}\frac{\cosh\frac{1}{kL_\rho}(kh+ky)}{\cosh\frac{kh}{kL_\rho}}, & -h \le y \le 0 \end{cases} \tag{2}$$

$$u^0(y) = \begin{cases} U_h - \frac{\Delta U}{2}\frac{\cosh\frac{1}{kL_\rho}(kh-ky)}{\cosh\frac{kh}{kL_\mathrm{v}}}, & 0 \le y \le h \\ U_l + \frac{\Delta U}{2}\frac{\cosh\frac{1}{kL_\rho}(kh+ky)}{\cosh\frac{kh}{kL_\mathrm{v}}}, & -h \le y \le 0 \end{cases}. \tag{3}$$

Here $\Delta\rho = \rho_h - \rho_l$, $\Delta U = U_h - U_l$, L_d and L_v are the density and velocity gradients scale lengths, respectively. $U_h(U_l)$ is velocity away from the interface in $x-$direction of the upper (lower) fluid and $\rho_h(\rho_l)$ is the density away from the interface of the upper (lower) fluid. Also the eigenfunction are given as (see Mikaelian 1990, 1996):

$$u_y^1(y) = \begin{cases} \left(\sigma + iku_x^{(0)}(y)\right)\frac{\sinh(kh-ky)}{\sinh kh}, & 0 \le y \le h, \\ \left(\sigma + iku_x^{(0)}(y)\right)\frac{\sinh(kh+ky)}{\sinh kh}, & -h \le y \le 0 \end{cases} \tag{4}$$

Here $A_T = \frac{\rho_h-\rho_l}{\rho_h+\rho_l} = \frac{1-r}{1+r}$ is Atwood number and $r = \frac{\rho_l}{\rho_h}(0 < r < 1)$ is the density ratio of the light fluid to the heavy one and $\zeta_1, \zeta_2, \zeta_3, \zeta_4, \zeta_5, \zeta_6$ are given, respectively by.

$$\zeta_1 = \coth(kh), \tag{6}$$

$$\zeta_2 = \frac{1}{\left(1+\frac{1}{kL_\rho}\right)\left(1-\frac{1}{kL_\rho}\right)}\left\{\coth(kh) - \frac{1}{kL_\rho}\tanh\left(\frac{kh}{kL_\rho}\right)\right\}, \tag{7}$$

$$\zeta_3 = \frac{1}{\left(1+\frac{1}{kL_\mathrm{v}}\right)\left(1-\frac{1}{kL_\mathrm{v}}\right)}\left\{\coth(kh) - \frac{1}{kL_\mathrm{v}}\tanh\left(\frac{kh}{kL_\mathrm{v}}\right)\right\}, \tag{8}$$

$$\zeta_4 = \frac{1}{\left(1+\frac{2}{kL_\mathrm{v}}\right)\left(1-\frac{2}{kL_\mathrm{v}}\right)}\left\{\coth(kh) - \frac{2}{kL_\mathrm{v}}\tanh\left(\frac{kh}{kL_\mathrm{v}}\right)\right\}, \tag{9}$$

$$\zeta_5 = \frac{\left[\begin{array}{c} \left\{\coth(kh) - \frac{1}{kL_\rho}\tanh\left(\frac{kh}{kL_\rho}\right) + \frac{1}{kL_\mathrm{v}}\tanh\left(\frac{kh}{kL_\mathrm{v}}\right)\right\} \\ \left\{\coth(kh) + \frac{1}{kL_\rho}\tanh\left(\frac{kh}{kL_\rho}\right) - \frac{1}{kL_\mathrm{v}}\tanh\left(\frac{kh}{kL_\mathrm{v}}\right)\right\} \\ \left\{\coth(kh) - \frac{1}{kL_\rho}\tanh\left(\frac{kh}{kL_\rho}\right) - \frac{1}{kL_\mathrm{v}}\tanh\left(\frac{kh}{kL_\mathrm{v}}\right)\right\} \end{array}\right]}{\left(1+\frac{1}{kL_\rho}+\frac{1}{kL_\mathrm{v}}\right)\left(1-\frac{1}{kL_\rho}+\frac{1}{kL_\mathrm{v}}\right)\left(1+\frac{1}{kL_\rho}-\frac{1}{kL_\mathrm{v}}\right)\left(1-\frac{1}{kL_\rho}-\frac{1}{kL_\mathrm{v}}\right)}, \tag{10}$$

Then, substituting in the product integration of Equation (1), the dispersion relation of KHI for two superimposed finite-thickness fluid layers maybe written as follows

$$\begin{aligned} &\left\{\sigma^2 + ik\left[(1-A_T)U_l + (1+A_T)U_h\right]\sigma\right. \\ &-\frac{k^2}{2}\left\{(1-A_T)U_l^2 + (1+A_T)U_h^2\right\}\zeta_1 \\ &+A_T(\Delta U)(ik^2)\left\{n + ik\frac{(U_2+U_1)}{2}\right\}\zeta_2 \\ &-(\Delta U)(ik^2)\left\{nA_T + ik\frac{\rho_2U_2 - \rho_1U_1}{\rho_1+\rho_2}\right\}\zeta_3 \\ &-k^3\frac{(\Delta U)^2}{4}\zeta_4 + A_T(ik^2\Delta U)\left\{n + ik\frac{(U_1+U_2)}{2}\right\}\zeta_5 \\ &\left.-kgA_T\zeta_6 = 0. \right. \end{aligned} \tag{5}$$

$$\zeta_6 = \frac{1}{(kL_\rho+1)(kL_\rho-1)}\left\{kL_\rho\coth(kh) - \tanh\left(\frac{kh}{kL_\rho}\right)\right\}. \tag{11}$$

At $kh \to \infty$, one can see that $\zeta_1 = 1, \zeta_2 = 1 + \frac{1}{kL_\rho}, \zeta_3 = 1 + \frac{1}{kL_\mathrm{v}}, \zeta_4 = 1 + \frac{2}{kL_\mathrm{v}}, \quad \zeta_5 = 1 + \frac{1}{kL_\rho} + \frac{1}{kL_\mathrm{v}}$ and $\zeta_6 = kL_\rho + 1$, in this case the dispersion relation (5) reduces to the same equation obtained earlier by Wang *et al.* (2009, 2010) in the limiting case of two-dimensional disturbances. While at $kL_\mathrm{v} = kL_d = 0$, one can see that $\zeta_2 = \zeta_3 = \zeta_4 \quad = \zeta_5 = 0$ and $\zeta_6 = 1$. Therefore Eq. (5) becomes $\frac{\sigma^2}{kg} = \frac{\rho_h-\rho_l}{(\rho_h+\rho_l)\coth(kh)}$, which agrees with Eq. (10) in Mikaelian (1990) in the absence of the surface tension and at $t_1 = t_2 = h$.

To discuss the roles played by the density and velocity gradients on the linear growth rate γ and the frequency ω, the dispersion relation (5) has been solved about the eigenvalue $\sigma = \gamma - i\omega$. In this case, both ω and γ, respectively, are

$$\frac{2\omega}{k\Delta U} = 2\left\{\frac{1-r}{1+r} + \frac{U_2+U_1}{\Delta U}\right\} - \left\{\frac{1-r}{1+r}\right\}\left\{\frac{\zeta_2+\zeta_3-\zeta_5}{\zeta_1}\right\}, \quad (12)$$

$$\left(\frac{2\gamma}{k\Delta U}\right)^2 = 1 - \left(\frac{1-r}{1+r}\right)^2 + 2\left(\frac{1-r}{1+r}\right)^2\frac{\zeta_2}{\zeta_1} - 2\left\{1-\left(\frac{1-r}{1+r}\right)^2\right\}\frac{\zeta_3}{\zeta_1} + \frac{\zeta_4}{\zeta_1} - 2\left(\frac{1-r}{1+r}\right)^2\frac{\zeta_5}{\zeta_1} - \left(\frac{1-r}{1+r}\right)^2\left\{\frac{\zeta_2+\zeta_3-\zeta_5}{\zeta_1}\right\}^2 + \frac{g}{k}\left(\frac{1-r}{1+r}\right)\left(\frac{\Delta U}{2}\right)^2\frac{\zeta_6}{\zeta_1}. \quad (13)$$

In our analysis, both of the density and velocity gradients are not equal 1 (i. e. $kL_\rho \neq 1, kL_u \neq 1$)).

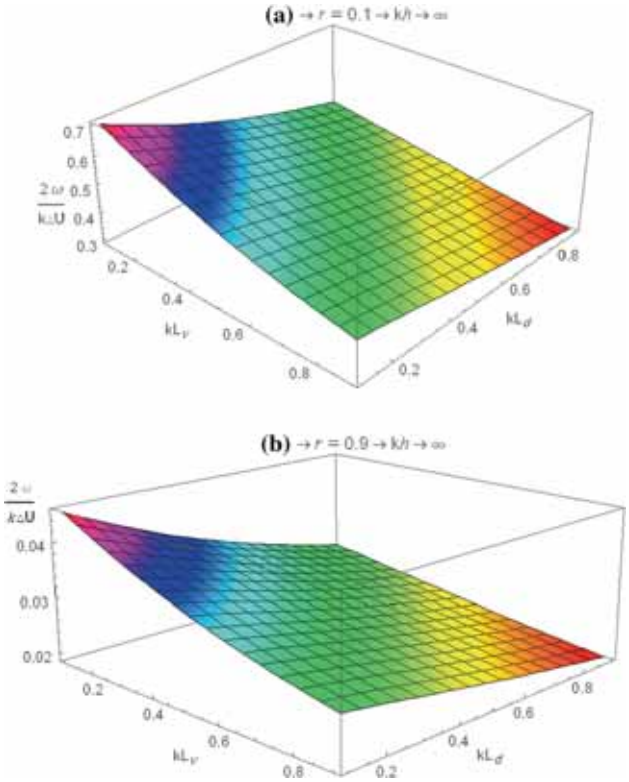

Figure 2. The role of density and velocity gradients in $2\omega_{KHI}/k\Delta U$ with $kh \to \infty$ (**a**) at $r = 0.1$, (**b**) at $r = 0.9$.

3. Results and discussions

The combined role of velocity and density gradients on the behavior of normalized frequency at $kh \to \infty$(two semi-infinite layers) has been studied by Wang *et al.* (2009, 2010). They showed that both the velocity and density gradients have a stabilizing effect on the behavior of frequency of KHI. This role has been once again presented in Fig. (2) from Eq. (12) at $kh \to \infty$, but at the constant values of $r = \rho_l/\rho_h$ ($r = 0.1, 0.9$ and $U_l = -1, U_h = 1$, where the normalized frequency at $kL_v = kL_d = 0$ is $\frac{2\omega}{k\Delta U} = \frac{U_h+U_l}{\Delta U} + \frac{1-r}{1+r}$ and at $U_h = 1, U_l = -1$, we get $\left(\frac{2\omega}{k\Delta U}\right)_{r=0.1} = 0.8181$, $\left(\frac{2\omega}{k\Delta U}\right)_{r=0.9} = 0.053$).

In Fig. 2, one can see that the values of normalized frequency $\frac{2\omega(L_d,L_v)}{k\Delta U}$ as a function of both the velocity and density gradients at $r = 0.1, 0.9$ are less than their counterparts in the absence of them (i.e. $\frac{2\omega(L_d=L_v=0)}{k\Delta U} = 0.8181, 0.053$, respectively). This implies that, the presence of both velocity and density gradients tends to stability role on the behaviour of normalized frequency. This role increases as the velocity and density gradient increase.

The combined role of velocity and density gradients on the behavior of normalized frequency of two finite-thickness fluid (Eq.12) layers has been presented in Fig. 3, where the normalized frequency is plotted among the normalized thicknesses of the density transition layer and the thickness of velocity shear layer at $kh = 10$, $r = 0.1, 0.9$, respectively. One can see that, the values of $2\omega_{KHI}/k\Delta U$ in Fig. 3(a) at $kh = 10$ are less than their counterparts in Fig. 2(a) at $kh \to \infty$. This indicates that, the values of normalized frequency of KHI for two finite-thickness fluid layers are less than their counterparts in the case of two semi-infinite fluid layers. The same phenomenon hold in Fig. 3(b) at $r = 0.9$, where the values of normalized frequency in Fig. 3(b) at $kh = 10$ are less than their counterparts in Fig. 2(b) at $kh \to \infty$. Now, if we compare between the values of normalized frequency in Fig. 3(a) at $r = 0.1$ and in Fig. 3(b) at $r = 0.9$. It can be seen that the values of normalized frequency in Fig. 3(b) are less than their counterparts in Fig. 3(a). This implies that the values of normalized frequency decrease as the density ratio of the light fluid to the heavy one increases for a system consisting of two finite-thickness fluid layers.

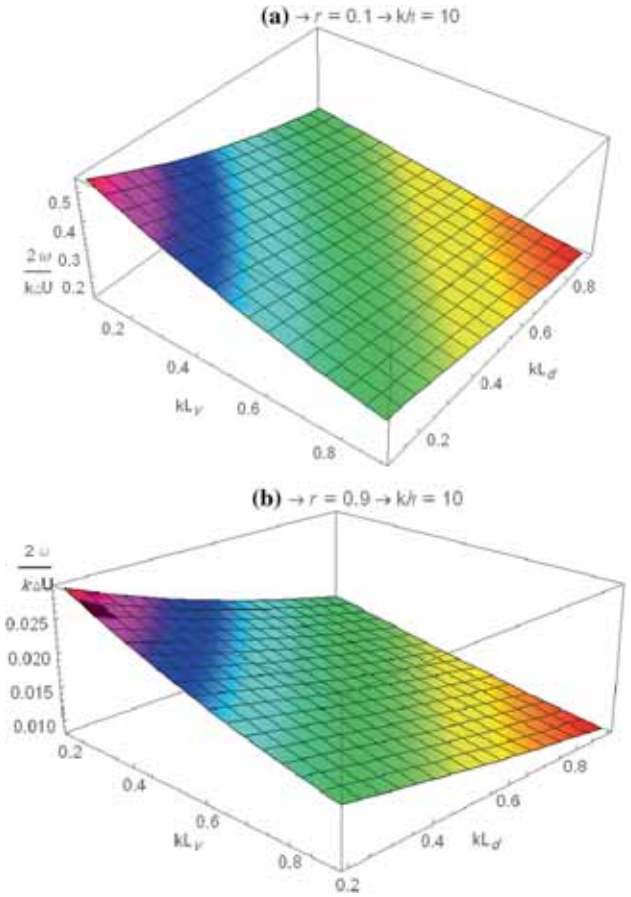

Figure 3. The role of density and velocity gradients in $2\omega_{KHI}/k\Delta U$ with $kh = 10$ (**a**) at $r = 0.1$, (**b**) at $r = 0.9$.

Now, to see the effects of various parameters included in the analysis on the linear normalized growth rate of KHI of the system under consideration, we draw the square of normalized growth rate $(2\gamma/k\Delta U)^2$ in Eq. (13) at $g = 0$, versus the normalized thicknesses of the density transition layer (kL_d) and the normalized thickness of velocity shear layer (kL_v), each one separately or together, for various values of the thickness of the two layers (i.e. $kh \to \infty$, $kh = 10$) at $r = 0.1, 0.9$, where the classical square normalized growth rate of KHI given as $(\frac{2\gamma}{k\Delta U})^2_{classical} = 1 - \left(\frac{1-r}{1+r}\right)^2$ at $g = 0$, and at $r = 0.1, 0.9$ is $(\frac{2\gamma}{k\Delta U})^2_{classical}(r = 0.1) = 0.33$ and $(\frac{2\gamma}{k\Delta U})^2_{classical}(r = 0.9) = 0.99$.

The effect of velocity gradient only (i. e. $kL_d = 0$) in $(2\gamma/k\Delta U)^2$ has been presented in figures (4) and (5). In Fig. (4) the square normalized growth rate is plotted against the density ratio ($r = \frac{\rho_l}{\rho_h}$) at $kh \to \infty$(the case of two semi-infinite fluid layers) for different values of the velocity gradient $kL_v = 0, 0.2, 0.4, 0.8$. It is shown that, the values of $(2\gamma/k\Delta U)^2$ in the presence of velocity gradient are less than their counterparts in case of classical KHI ($kL_v = 0$). Also the values of square normalized growth rate $(2\gamma/k\Delta U)^2$ decreases as kL_v increases. While the values of square normalized growth rate $(2\gamma/k\Delta U)^2$ increase as the values of r increase.

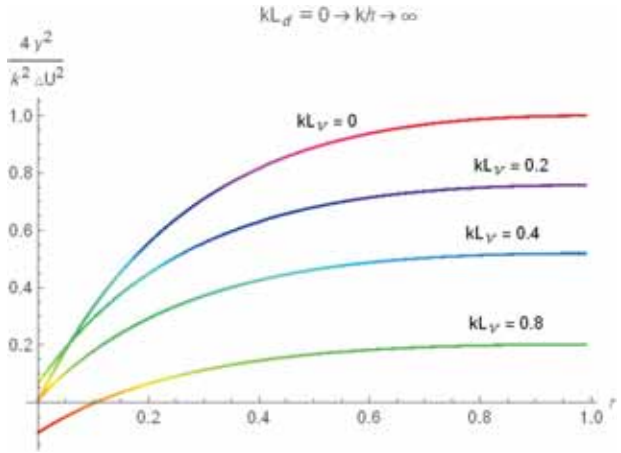

Figure 4. The role of velocity gradient (kL_v) at $0, 0.2, 0.4, 0.8$ and $kL_d = 0, kh \to \infty$.

In Fig. 5(a) and (b), we show the square normalized growth rate against the velocity gradient and the density ratio ($r = \frac{\rho_l}{\rho_h}$) at $kh \to \infty$ and $kh = 10$ (the case of two finite-thickness fluid layers). As shown in Fig. 5(b), the values of $(2\gamma/k\Delta U)^2$ are less than their counterparts in Fig. 5(a). This implies that the values of normalized growth rate of KHI under the effect of the velocity gradient only and for two finite-thickness fluid layers are less than their counterparts for two semi-infinite fluid layers.

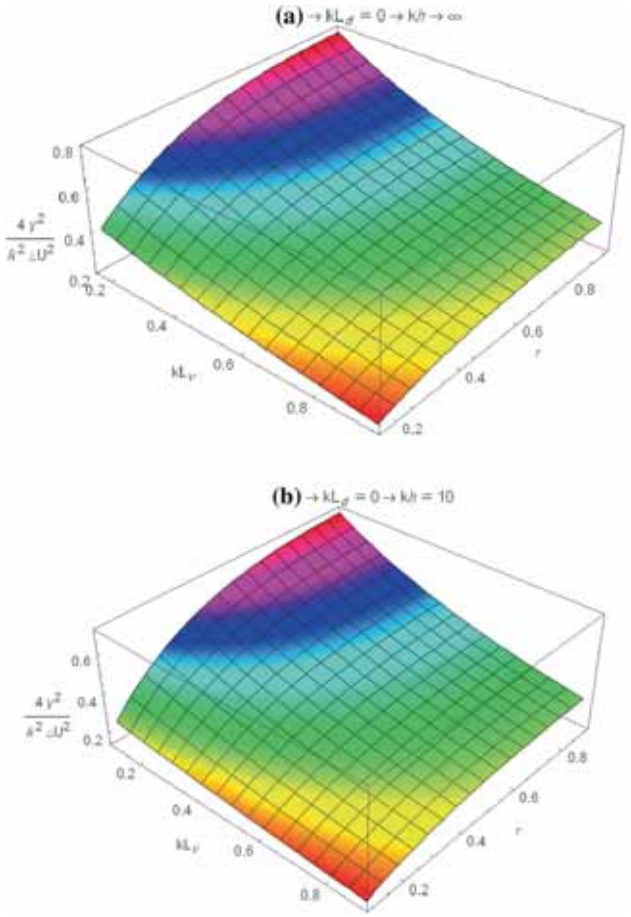

Figure 5. The relation among $(2\gamma/k\Delta U)^2$,$kL_{\rm v}$ and density ratio ($r = \rho_l/\rho_h$) with $kL_d = 0$, (**a**) at $kh \to \infty$, (**b**) at $kh = 10$.

The role of density gradient only (i. e. $kL_v = 0$) on the normalized growth rate has presented in figures 6 and 7. In Fig. 6 the square normalized growth rate is plotted against the density ratio ($r = \rho_l/\rho_h$) at $kh \to \infty$(the case of two semi-infinite fluid layers) for different values of the density gradient $kL_d = 0, 0.2, 0.4, 0.8$. It is shown that, the values of $(2\gamma/k\Delta U)^2$ in the presence of density gradient are greater than their counterparts in case of classical KHI ($kL_d = 0$). These values increase as kL_d increases for small values of the density ratio (r). While this differ gradually declines with the increase in density ratio r, and at the great values of r the square normalized growth rate has the same values for all different values of the density gradient (kL_d).

In Fig. 7(a) and (b), we show the square normalized growth rate against the density gradient and the density ratio ($r = \rho_l/\rho_h$) at $kh \to \infty$ and $kh = 10$, respectively. It can be seen that, the values of square normalized growth rate in the case of two

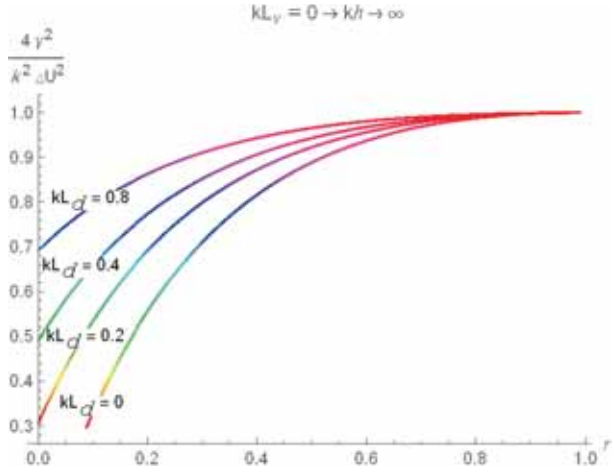

Figure 6. The role of density gradient (kL_d) at 0, 0.2, 0.4, 0.8 and $kL_{\rm v} = 0$, $kh \to \infty$.

finite-thickness fluid layers do not show any noticeable change from their counterpart of two semi-infinite fluid layers, where the values of $(2\gamma/k\Delta U)^2$ are almost equal.

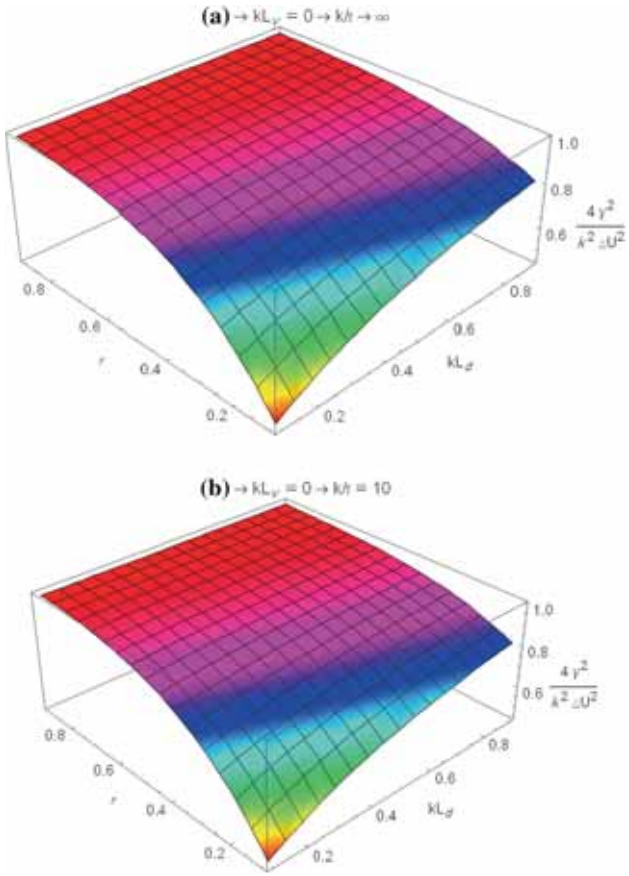

Figure 7. The relation among $(2\gamma/k\Delta U)^2$, kL_d and density ratio ($r = \rho_l/\rho_h$) with $kL_{\rm v} = 0$, (**a**) at $kh \to \infty$, (**b**) at $kh = 10$.

The combined effect of both velocity and density gradients in $(2\gamma/k\Delta U)^2$ is identical as shown in Eq. (13) is presented in figures 8 and 9 at $kh = 10$, $kh \to \infty$ and $r = 0.1, 0.9$.

In Fig. 8(a) at $r = 0.1$ and $kh = 10$, it can see that the values of $(2\gamma/k\Delta U)^2$ are less than their counterparts in the case of classical KHI $(\frac{2\gamma}{k\Delta U})^2_{classical}(r = 0.1) = 0.33)$ at the large values of velocity gradient and the small values of density gradient and vice versa. This implies that, the behavior of normalized growth rate in the case of two finite fluid layers at the small values of density ratio (r) capitulates to the effect of velocity gradient (stabilizing effect) in the case of large velocity and small density gradients values. While it capitulates to the effect of density gradient (destabilizing effect) in the case of small velocity and larger density gradients values.

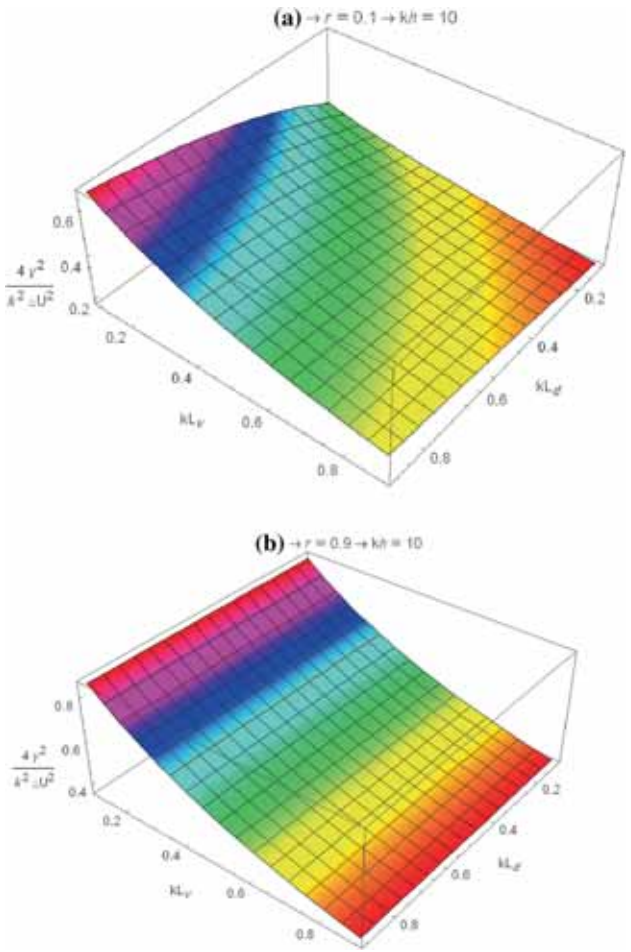

Figure 8. The role of density and velocity gradients in $(2\gamma/k\Delta U)^2$ with $kh = 10$, (**a**) at $r = 0.1$), (**b**) at $r = 0.9$.

In Fig. 8(b) and at $r = 0.9$, $kh = 10$, one can see that, the values of $(2\gamma/k\Delta U)^2$ are less than their counterparts in the case of classical KHI$(\frac{2\gamma}{k\Delta U})^2_{classical}(r = 0.9) = 0.99)$. This implies that, the behavior of normalized growth rate for the case of two semi-infinite fluid layers capitulates to the effect of velocity gradient (stabilizing effect) in the case of large density ratio (r) values. These values decrease as the velocity gradient increases, while it does not show any noticeable change with the increase in the density gradient values.

In Fig. 9(a) and (b), the square of normalized growth rate is plotted against both the velocity and density gradients at $kh \to \infty$ and $r = 0.1, 0.9$, respectively. it shown that the values of square of normalized growth rate in Fig. 9 (at $kh \to \infty$) are greater than their counterparts in Fig. 8 (at $kh = 10$). Which implies that, under the effect of density and velocity gradients the KHI model of two finite fluid layers is more stability than the KHI model of two semi-infinite fluid layer.

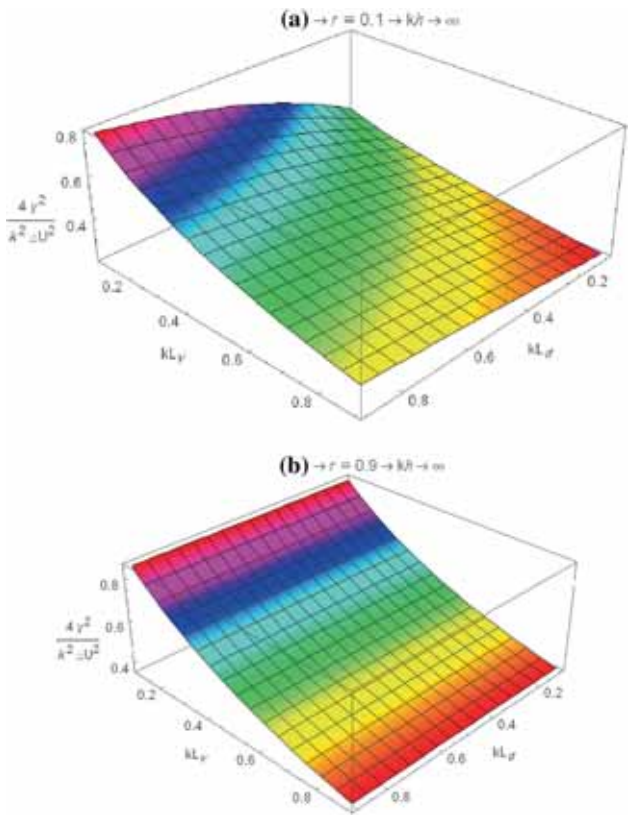

Figure 9. The role of density and velocity gradients in $(2\gamma/k\Delta U)^2$ with $kh \to \infty$, (**a**) at $r = 0.1$, (**b**) at $r = 0.9$.

Again, the combined effect of both velocity and density gradients but in γ is presented in figures 10 and 11 at $kh = 5, 10$, $kh \to \infty$ and $r = 0.1, 0.9$, respectively. From these figures, it can see that the values of γ increase as the values kh increase. Also, one can see that in Fig. 10 and at $r = 0.1$ the values of

γ are less than their counterparts in the case of classical KHI ($\gamma_{classical}(r = 0.1) = 0.5744$) just at the large values of velocity gradient and the small values of density gradient. While in Fig. 11 and at $r = 0.9$, one can see that, the values of γ are less than their counterparts in the case of classical KHI ($\gamma_{classical}(r = 0.9) = 0.995$) at all values of both velocity and density gradients.

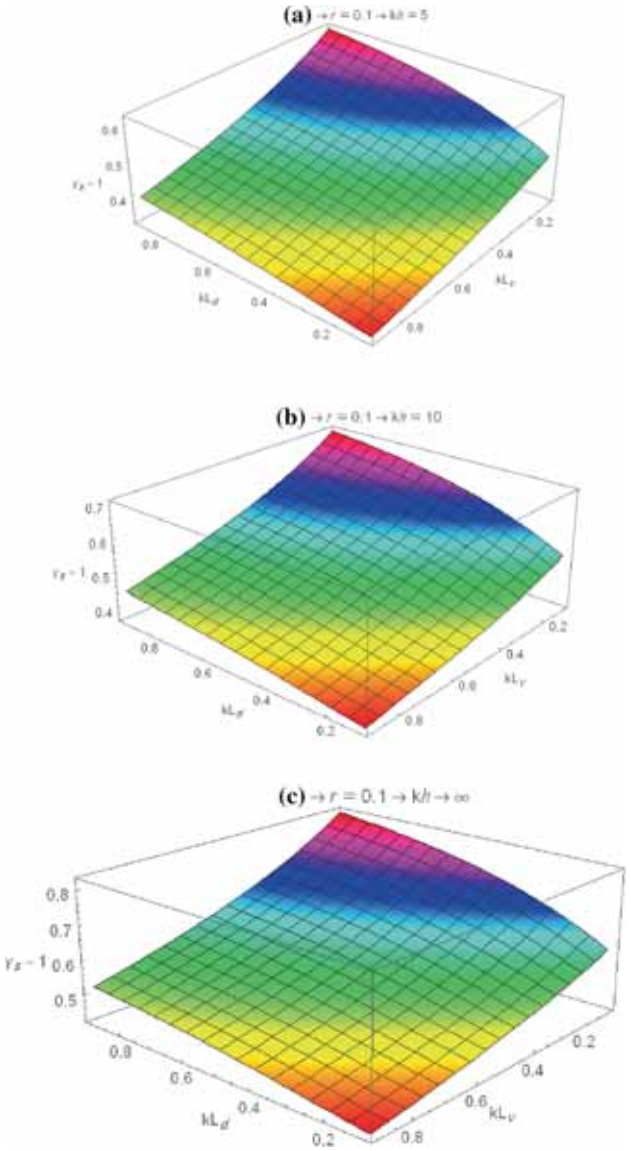

Figure 10. The role of density and velocity gradients in γ with $r = 0.1$, $U_h = 1, U_l = -1$ (**a**) at $kh = 5$, (**b**) at $kh = 10$, (**c**) at $kh \to \infty$.

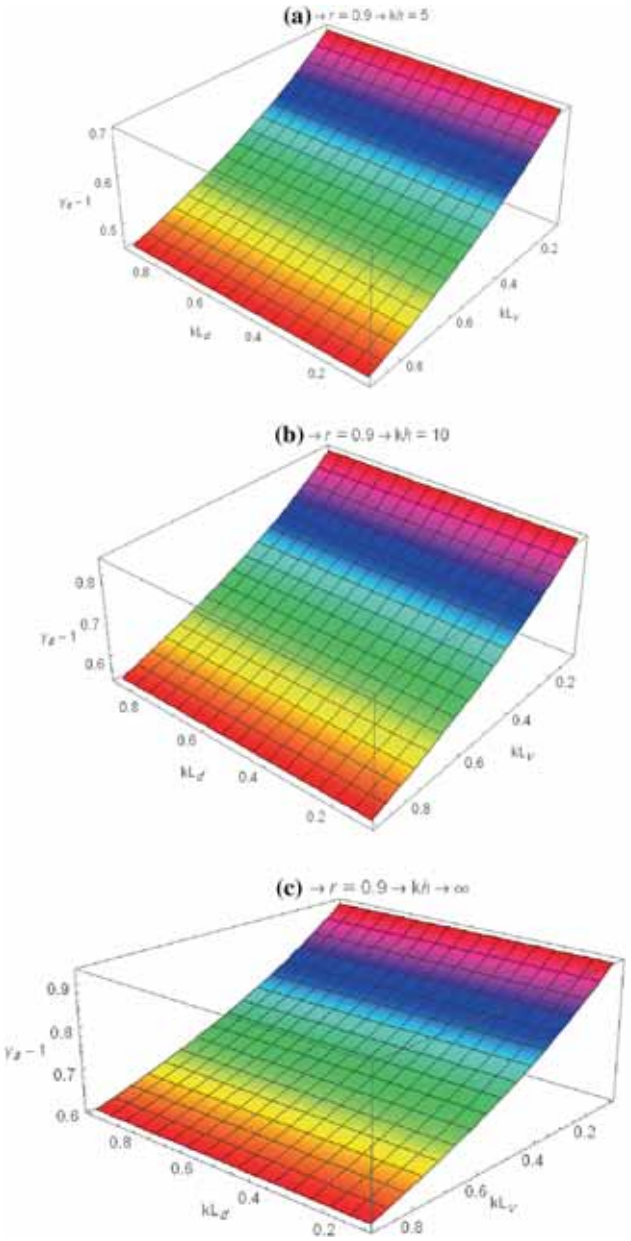

Figure 11. The role of density and velocity gradients in γ with $r = 0.9$, $U_h = 1, U_l = -1$ (**a**) at $kh = 5$, (**b**) at $kh = 10$, (**c**) at $kh \to \infty$.

Using the definition formula $\tau_{KH} = \frac{2\pi}{\gamma_{KH}}$, the combined effect of both velocity and density gradients of the KHI instability is presented in figures 12 and 13 at $kh = 10, kh \to \infty$ and $r = 0.1, 0.9$, respectively. From these figures, it can see that the values of τ_{KH} decrease as the values kh increase.

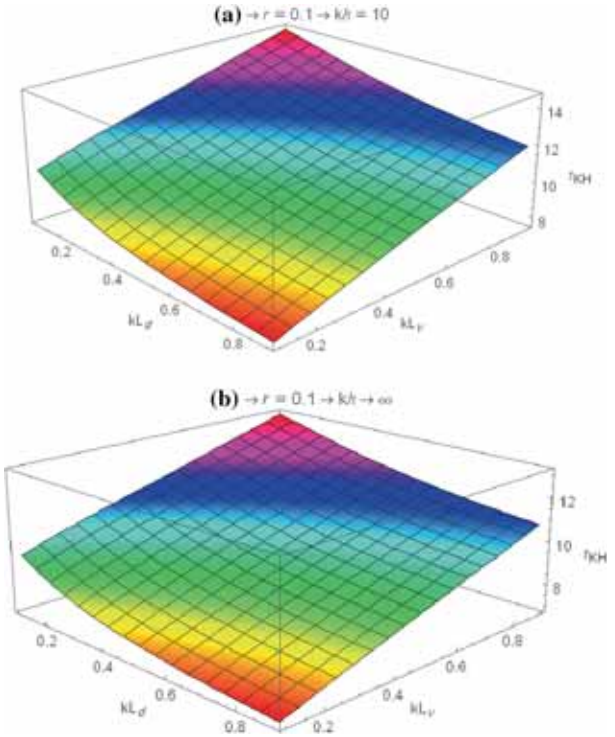

Figure 12. The role of density and velocity gradients in τ_{KH} with $r = 0.1$, $U_h = 1$, $U_l = -1$, (**a**) at $kh = 10$, (**b**) at $kh \to \infty$.

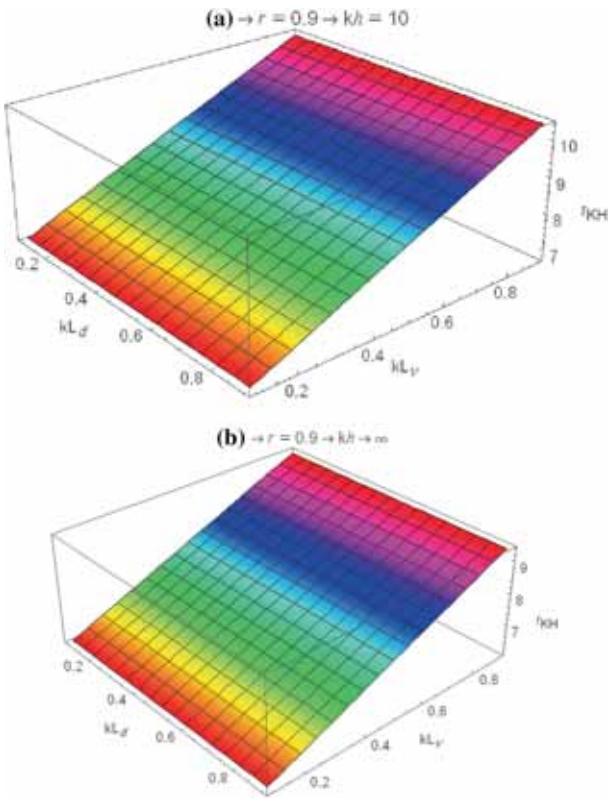

Figure 13. The role of density and velocity gradients in τ_{KH} with $r = 0.9$, $U_h = 1$, $U_l = -1$, (**a**) at $kh = 10$, (**b**) at $kh \to \infty$.

In Fig. 12 and at $r = 0.1$ we can see that, the values of τ_{KH} are less than their counterparts in the case of classical KHI ($\tau_{classical}(r = 0.1) = 10.9387$) just at the large values of velocity gradient and the small values of density gradient. While in Fig. 13 and at $r = 0.9$, the values of τ_{KH} are greater than their counterparts in the case of classical KHI($\tau_{classical}(r = 0.9) = 6.315$) at all values of both velocity and density gradients.

In this current communication, the combined effect of velocity and density gradients on the Kelvin–Helmholtz instability of two finite-thickness fluid layers have been studied. The linear normalized frequency and normalized growth rate are obtained. They numerically solved as a function of the density ratio for different values of the thickness of the two layers. The main results are listed below.

- Under the effect of velocity gradient only, the behaviour of growth rate capitulates to the stabilizing effect of velocity gradient
- Under the effect of density gradient only, the behaviour of growth rate capitulates to the destabilizing effect of density gradient.
- Under the effect of both velocity and density gradients together, the behaviour of growth rate capitulates to the stabilizing effect of velocity gradient in the case of large density ratio. While in case of small density ratio, the behavior of normalized growth rate capitulates to the effect of velocity gradient (stabilizing effect) just in the case of large velocity and small density gradients values, and it capitulates to the effect of density gradient (destabilizing effect) in the case of small velocity and larger density gradients values.
- Both the normalized frequency and normalized growth rate are undefined at $kL_{\mathrm{v}} = 1 \mathrm{or}\, kL_d = 1$.

Generally, both the values of normalized frequency and normalized growth rate for our selected model are less than their counterparts in the case of two semi-infinite fluid layers. This model is helpful to understand the formation mechanism of astrophysical jets and jet-like long spike in high-energy density physics (HEDP).

Acknowledgements

The authors would like to thank the reviewers for their thorough review. The authors highly appreciate the reviewers' comments and suggestions which significantly contributed to improving the quality of the publication.

References

Alexakis A., Young Y., Rosner R. 2002, Phys. Rev. E, 65, 026313
Chandrasekhar S. 1961, Hydrodynamic and Hydromagnetic Stability, Oxford University, London, p. 481
Chong R., Lafitte O., Cahen J. 2008, Phys. Scr, T132, 014039
Drake R. P. 2005, Plasma Phys. Control. Fusion, 47, 419
Gan Y., Xu A., Zhang G., Li Y. 2011, Phys. Rev. E, 83, 056704
Harding E. C. and Hansen J. F. 2009, Phys. Rev. Lett., 103, 045005
Harding E. C. *et al.* 2010, Phys. Plasmas, 17, 056310
Hurricane O. A. *et al.* 2009, Phys. Plasmas, 16, 056305.
Helmholtz H. L. F. 1868, Sitz. ber. Preuss. Akad. Wiss. Berlin. Phil.-Hist. Kl, 23, 215
Kelvin L (Thomson W. T.) 1871, Philos. Mag., 42, 362
Khenner M. V., Lyubimov D. V., Belozerova T. S., Roux B. 1999, Eur. J. Mech. B Fluid, 18, 1085
Kuridze D., Zaqarashvili T. V., Henriques V., Mathioudakis M., Keenan F. P., Hanslmeier, A. 2016, ApJ, 830, 133
Mohamed A. A., Elhefnawy A. R. F., Mahmoud Y. D. 1994, Physica A, 202, 264
Mikaelian K. O. 1990, Phys. Rev. A, 42(12) 7211
Mikaelian K. O. 1996, Phys. Rev. E, 54(4) 3676
Raj R., Guha A. 2017, arXiv:1710.07910v1
Remington B. A., Drake R. P., Ryutov D. D. 2006, Rev. Mod. Phys., 78, 755
Wang L. F., Xue C., Ye W. H., Li Y. J. 2009, Phys. Plasmas, 16, 112104
Wang L. F., Ye W. H., Li Y. J. 2010, Phys. Plasmas, 17, 042103
Ye W. H., Wang L. F., Xue C., Fan Z. F., He X. T. 2011, Phys. Plasmas, 18, 022704
Zaqarashvili T. V., Vörös Z., Zhelyazkov I. 2014, A & A, 561, A62
Zaqarashvili T. V., Zhelyazkov I., Ofman L. 2015, ApJ, 813, 123
Zhelyazkov I. 2015, J. Astrophys. Astr., 36, 233